Dislocation dynamic modelling of the brittle-ductile transition in tungsten

Edmund Tarleton, Steve G Roberts

Dislocation dynamic modelling of the brittle-ductile transition in tungsten

Journal:	*Philosophical Magazine & Philosophical Magazine Letters*
Manuscript ID:	TPHM-08-Oct-0359.R1
Journal Selection:	Philosophical Magazine
Date Submitted by the Author:	25-Mar-2009
Complete List of Authors:	Tarleton, Edmund; University of Oxford, Materials Roberts, Steve; University of Oxford, Materials
Keywords:	brittle-ductile transition, cracks, dislocation dynamics, dislocations, fracture
Keywords (user supplied):	brittle-ductile transition, cracks, dislocation dynamics

Philosophical Magazine
Vol. 00, No. 00, 00 Month 200x, 1–10

RESEARCH ARTICLE

Dislocation dynamic modelling of the brittle-ductile transition in tungsten

E. Tarleton* and S.G. Roberts

Department of Materials, Oxford University, Parks Road, Oxford, OX1 3PH, UK;

(*received October 2008*)

Brittle-ductile transitions in metals, ceramics and semiconductors are closely connected with dislocation activity emanating near to crack-tips. We have simulated the evolution of crack-tip plasticity using a two dimensional dislocation dynamics model which has been developed to include two symmetric slip planes intersecting the crack-tip, and applied to single-crystal tungsten. The dislocation mobility law used was physically based on double-kink nucleation on screw dislocations, with an activation energy reduced by the local stress. Even in the strong stress gradients near a crack tip, the dislocations are found to self-organise so that the internal stress in the array is effectively constant with time and position over a wide range of strain rates and temperatures. The resultant net activation energy for dislocation motion is found to be constant and close to the activation energy experimentally measured for the brittle-ductile transition. Use of a fracture criterion based on the local crack-tip stress intensity factor, as modified by the stresses from the emitted dislocations, allows explicit prediction of the form and temperature of the brittle-ductile transition. Predictions are found to be in very close agreement with experiment.

Keywords: ductile-brittle transition; dislocation dynamics; BDT; fracture; brittle-ductile transition; cracks; dislocation shielding

1. Introduction

Many materials are brittle at low temperatures and ductile at high temperatures. The temperature at which the fracture mode changes, the brittle-ductile transition (BDT) temperature, T_{BDT}, depends on both strain rate and loading geometry.

The basic parameter controlling fracture is the stress intensity factor, K, which characterises the form and extent of the stress concentration around a loaded crack. For simple geometries, $K = \alpha\sigma\sqrt{\pi c}$, where σ is the remote tensile stress acting on a crack of length c, and α is a geometrical factor ≈ 1.

If the stress intensity at the crack tip K_{tip} exceeds the critical value required for fracture, (the Griffith value for a mode I crack, K_{Ic})

$$K_{tip}(t) \geq K_{Ic} \tag{1}$$

the material will break in a brittle manner. The value of the applied stress intensity factor, K_{app}, at which (1) occurs is the fracture value, K_{frac}:

$$K_{frac} = K_{app}(t) \quad \text{at which} \quad K_{tip}(t) = K_{Ic}. \tag{2}$$

*Corresponding author. Email: edmund.tarleton@oriel.ox.ac.uk

ISSN: 1478-6435 print/ISSN 1478-6443 online

DOI: 10.1080/1478643YYxxxxxxxx
http://www.informaworld.com

The brittle-ductile transition arises because of a competition between the rate at which the stress intensity at a crack increases because of increasing the applied loading, K_{app}, and the rate at which it decreases because of the effect of dislocations active near the crack-tip.

Experiments on almost all materials which exhibit a brittle-ductile transition have shown that as the temperature is increased, up to T_{BDT}, the applied stress intensity required for fracture, K_{frac}, also increases [1–4]; this is associated with an increase in crack-tip dislocation activity [5]. If no dislocations are present condition (1) is met when $K_{tip}(t) = K_{app}(t)$; this corresponds to totally brittle fracture. As the strain rate is lowered or the temperature is raised, dislocations may be nucleated at or near the crack-tip and move away from their sources, allowing other dislocations to be produced. Arrays of dislocations form along slip planes, and reduce the stress at the crack-tip (known as "dislocation shielding")[5], therefore:

$$K_{tip}(t) = K_{app}(t) - K_{dis}(t), \tag{3}$$

where K_{dis} is the dislocation shielding, due to the stress at the crack-tip exerted by the dislocations. If limited dislocation activity occurs, fracture occurs but with $K_{frac} > K_{Ic}$ due to the shielding effect of the dislocations. If sufficient dislocation activity occurs, the high level of K_{dis} can keep K_{tip} below the value required for fracture, so that condition (1) is never satisfied and the material is then ductile.

Here we show that a transition temperature can result naturally from the dynamics of dislocation generation and motion near the crack-tip. The force between dislocations decays only as $1/r$ and as more dislocations are nucleated, full 3-dimensional simulations become very computationally intensive. We therefore use a simpler 2D model which captures the essential processes which lead to the BDT and is able to predict transition temperatures; these we compare to experiments.

2. The Model

2.1. *Model Geometry*

To be able to model the emission of dislocations from a crack-tip over experimentally realistic time and length scales, it is useful to model the real 3-dimensional situation by using a 2-dimensional simulation (see figure 1). This approximation is justifiable if the crack front is effectively homogenous. This is likely to be the case if there is a high density of dislocation sources at or near the crack-tip. 3D simulations of a Frank-Read source close to a mode I crack using a modified version of the 3D dislocations dynamics code MicroMegas [6] have shown that if there is a high density of sources (equivalent to the periodic boundary conditions used in Micromegas: see figure 1 (a)) then the sources collectively produce straight parallel edge dislocations. These edge dislocations then move away from the source in an orderly fashion; shown in figure 1 (b). This situation can be approximated by modelling the plastic zone as an array of parallel dislocations, emanating from a line dislocation source near the crack-tip as shown in figure 1 (c) and (d). Observation by electron backscattered diffraction in the SEM of crack-tip plastic zones in single crystal tungsten, the material modelled here, figure 2, shows that the real crack-tip plastic zone corresponds very closely in geometry to those modelled, figure 1.

An advantage of a 2D model is that the distribution of image dislocations required for zero traction on the crack surfaces can be calculated by using the analytic expressions developed by Lakshmanan and Li [7] for an infinite crack under mode I loading. Given the position and Burgers vector of a dislocation the resulting

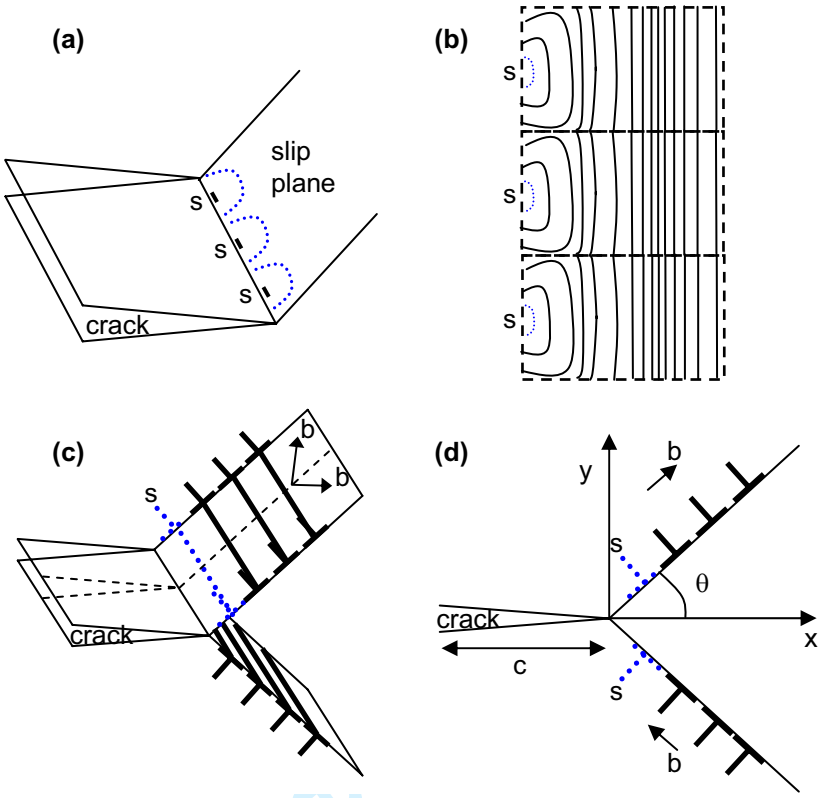

Figure 1. (a) Schematic of a 3-dimensional crack with multiple dislocation sources, s. (b) The sources produce dislocation half loops which combine to give parallel straight edge dislocations on the slip plane. (c) The 2D dislocation array modelled on two symmetric slip planes. (d) By cutting along the dashed line the 3D problem in (c) can be reduced to a 2D problem.

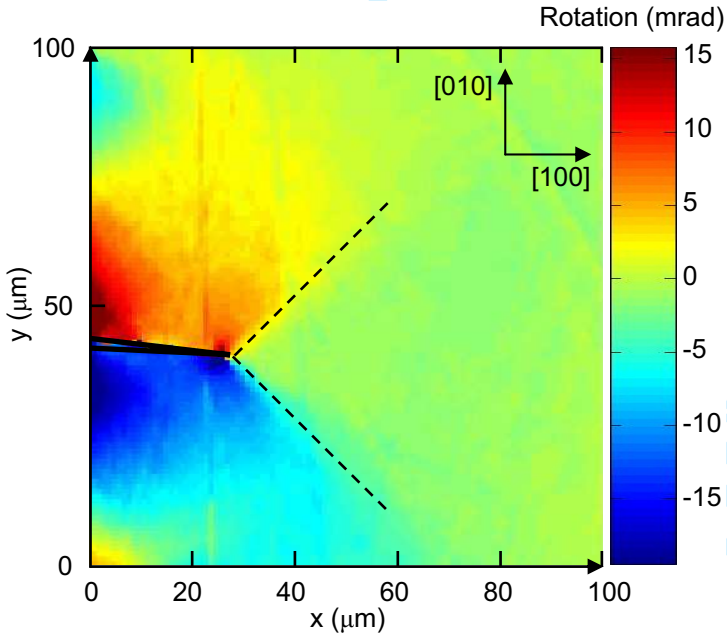

Figure 2. An EBSD image showing the rotation about the axis parallel to the crack front of a typical pre-cracked tungsten specimen used in the fracture tests modelled here. The rotation is induced by the strain field of the dislocations which are on {110} slip planes at ±45° to the crack tip plane. The majority of dislocation activity, visible by a rapid change in rotation, is located on the slip planes (indicated by dashed lines) intersecting the crack tip (indicated by a solid line). The applied load was $K_{app} = 6.4$ MPa m$^{1/2}$ applied at a strain rate of 2.9×10^{-6}s^{-1} at $T = 485$ K.

distribution of image dislocations and the resulting image stress on the dislocation can be calculated. As the image terms are linear they can be added to calculate the total image stress resulting from any number of dislocations.

This type of model has been successfully used to study crack-tip plasticity in various materials [5, 8–10]. However, while previous variants of this type of model, which used only one of the two slip planes shown in figure 1, were able to predict the rise in K_{frac} with temperature in a wide range of materials [10, 11], such models were unable to predict an explicit brittle-ductile transition. The model described here includes a symmetric slip plane below the crack-tip; the additional dislocation interactions and subsequent shielding changes the model's behaviour so that it intrinsically produces a brittle-ductile transition [12]. Here we give details of the model and use it to study pure single crystal tungsten, where a comprehensive set of experimentally measured BDT data is available [13] at five different strain rates. In the experiments, test specimens were in the form of pre-cracked four-point bend beams, with crystal axes $\langle 100 \rangle$ along the major axes of the beams. The primary slip systems in tungsten are $\{110\}\langle 1\bar{1}1 \rangle$; the slip planes with the highest critical resolved shear stress near the crack tip are those intersecting the crack tip, and at an angle of 45° to the crack plane as shown in figure 2 (i.e. the experimental geometry corresponds closely to that shown in figure 1 (d) with $\theta = 45°$). In the model (as in the experiments) the applied stress increases linearly in time, hence eventually the resolved shear stress on a test dislocation at the source at position r_0 is positive and a dislocation is produced and moves along the slip plane. The source feels a back stress from the dislocation which decreases as the dislocation moves away; also the stress on the source from the applied loading increases with time. Eventually $\tau(r_0) > 0$ again and another dislocation is nucleated. The process repeats and an array of moving dislocations is formed on each slip plane as illustrated in figure 1 (d).

The shear stress, τ_i, on the i^{th} dislocation in the array of dislocations is given by:

$$\tau_i = \frac{K_{app}}{r_i^{1/2}} f(\theta) + \frac{K_{app}}{c^{1/2}} g(r_i, \theta, c, L) + \sum_j^n h(r_i, r_j, \theta, \mu, \nu) + \sum_{j \neq i}^n m\left(|r_i - r_j|^{-1}, \theta, \mu, \nu\right) \tag{4}$$

where $K_{app} = K_{app}(t)$ is the applied stress intensity factor, $r_i = r_i(t)$ is the distance of the i^{th} dislocation from the tip of the crack (of length c), $n = n(t)$ is the number of nucleated dislocations, θ is the angle between the slip plane and the crack plane, μ is the material's shear modulus, ν is Poisson's ratio, L is the specimen thickness and f, g, h and m are functions of the variables given. The first term corresponds to the crack-tip stress field, the second term to the specimen's 'background' bending stress field, the third term to dislocation - image dislocation interactions and the fourth term to direct dislocation-dislocation interactions. For edge dislocations near a mode I crack, exact solutions for the first, third and fourth terms are given by Lakshmanan and Li [7]; the second term is simple to calculate for a given specimen geometry.

Dislocation dynamics modelling requires a velocity law for the dislocations. In bcc metals, such as tungsten, the screw dislocations move much more slowly than edge dislocations [14] so that the expansion of dislocation loops and hence the operation of dislocation sources is controlled by the mobility of the screw dislocations. Thus in the simulations, the mobility law used is one appropriate to screw dislocations moving by kink-pair nucleation and motion [15]

$$v(\tau, T) = v_0 \exp(-(Q - \tau V_A)/k_B T) \tag{5}$$

where Q is a constant representing the kink pair formation energy at zero stress, τ is shear stress at the dislocation position, $V_A = 2V_{kp}$ where V_{kp} is the activation volume for the kink pair formation, v_0 is a constant pre-factor and k_B is Boltzmann's constant. For tungsten, experiments [13, 16] found $Q = 1.75$ eV and a representative value [16–18] of V_a is $20b^3$ (where b is the Burgers vector magnitude); these values were used in the simulations reported here.

The local stress intensity at the crack-tip, $K_{tip}(t)$, is lower than the applied value, due to the elastic strain field of the dislocations "shielding" the crack-tip. The function for the stress intensity factor at the crack-tip has the form [7]

$$K_{tip}(t) = K_{app}(t) - K_{dis}(t) \tag{6}$$

$$= \dot{K}_{app}t - B\sum_{j=1}^{n(t)} r_i^{-1/2}(t) \tag{7}$$

$$\text{where} \quad B = \frac{3\mu b}{\sqrt{2\pi}(1-\nu)}\sin(\theta/2)\cos^2(\theta/2)$$

and θ is the slip plane angle; a derivation is given by Lakshmanan and Li [7]. The shielding from a given dislocation is proportional to $r^{-1/2}$; the sum over all dislocations, $n(t)$, gives the total shielding.

Fracture is assumed to occur when $K_{tip}(t) = K_{Ic}$, the critical value for pure cleavage fracture; see condition (1). Experimental work [12, 13] has found that once the crack starts to propogate it does so unstably and the fracture surface is seen to be planar cleavage. Modelling shows that once the crack extends even slightly, given a 'paired slip plane' type of plastic zone such as that modelled and observed, the shielding effect of the dislocations decreases and so such unstable crack propagation would be expected.

2.2. *Model Behaviour*

Typical results for the model, using input data (temperatures, loading rates and crack size) appropriate for the experiments on tungsten are shown in figure 3. The applied loading rate is constant whereas the shielding rate increases with time, because dislocations move away from the sources faster as the applied stress increases, giving rise to an increasing dislocation nucleation rate. This is illustrated in figure 3 (a): the nucleation rate increases continually while the plastic zone size growth rate reaches a peak value and then decreases. The dislocations are driven away from the crack-tip by the bending stress and the crack stress; both decrease as the dislocations move away from the crack tip. The net rate of increase in K_{dis} (see eqn (7)) is not constant but increases. Eventually the dislocation shielding rate exceeds the rate of applied deformation: $\dot{K}_{dis}(t) > \dot{K}_{app}(t)$ or

$$\frac{dK_{dis}}{dK_{app}} > 1 \tag{8}$$

so that K_{tip} reaches a maximum before decreasing (figure 3 (b)).

As the simulated temperature is increased the dislocations move away from the source faster, which increases the dislocation nucleation rate; the dislocation shielding K_{dis} increases and lowers K_{tip}. At a critical temperature the maximum value of K_{tip} is less than K_{Ic}: the fracture condition (1) is never met and the result of the simulation is then predicted to be ductile. The temperature at which this occurs

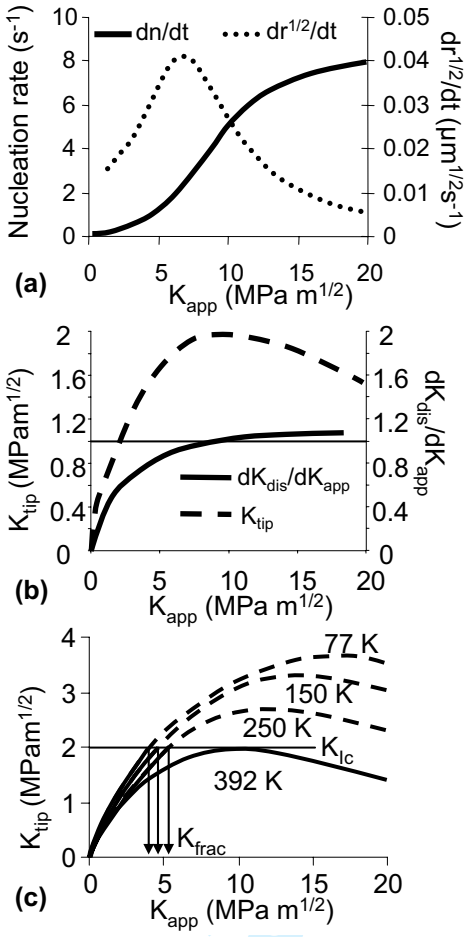

Figure 3. The origin of the BDT. (a) The derivatives, $dr^{1/2}/dt$ and dn/dt where r is the position of the leading dislocation and n the number of dislocations. The plastic zone size growth rate peaks whereas the dislocation nucleation rate continues to increase. (b) The dislocation shielding rate (solid line) increases; eventually $\dot{K}_{dis}$ exceeds $\dot{K}_{app}$ (horizontal line) producing a peak in K_{tip} (dashed line). The simulations in (a) and (b) used $T = 392$ K and $\dot{\varepsilon} = 2.9 \times 10^{-6}$ ms^{-1}. (c) Simulations for various temperatures. At higher temperatures K_{dis} increases, which lowers the peak stress intensity at the crack-tip K_{tip}. The BDT occurs when K_{tip} is lower than the critical stress intensity for cleavage, K_{Ic}. For this strain rate, this is 392 K.

is the brittle-ductile transition temperature, T_{BDT}.

2.3. *Modelling the BDT in tungsten*

The pre-factor v_0 in the dislocation velocity law (5) (the only parameter not derived from independent exeriments) was set by adjusting its value so that at the lowest strain rate used (2.9×10^{-6}s^{-1}) the predicted T_{BDT} matched the experimental T_{BDT} (392 K). All other parameters in the model: K_{Ic} (2MPa m$^{1/2}$) [19], $\dot{K} = (\pi c)^{1/2}\dot{\sigma}$, crack length c (60 μm), specimen thickness L (1 mm), and the slip plane angle θ (45°), were taken from experimental values [13]. (Note that the experimental strain rates given by Giannattasio et al [13] have been found to be miscalibrated by a constant factor; this miscalculation does not effect the conclusions of that study. The correct strain rates are given here and were used in the modelling.)

Figure 3(c) shows the critical condition for fixing v_0, which was adjusted for modelling the experiments at the lowest strain rate so that the maximum value of K_{tip} is just below K_{Ic}, at the experimental BDT temperature, so the material does not fracture and K_{frac} becomes infinite. At lower simulated temperatures

Table 1. The predicted transition temperatures and the experimentally measured values.

$\dot{\varepsilon}$ (s^{-1})	Predicted T_{BDT} (K)	Experimental [13] T_{BDT} (K)
3.3×10^{-3}	523	520
7.3×10^{-4}	491	478
7.3×10^{-5}	444	438
7.3×10^{-6}	406	409
2.9×10^{-6}	392[a]	392

[a]Velocity law prefactor fitted to match T_{BDT} value at this $\dot{\varepsilon}$.

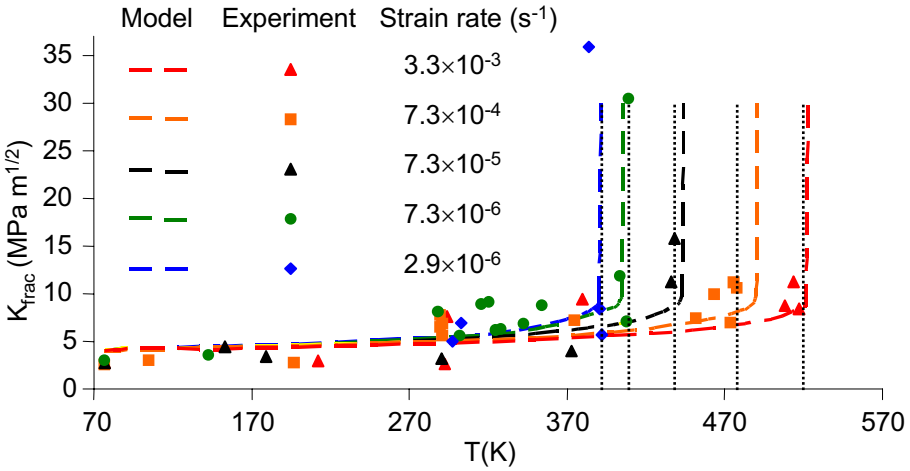

Figure 4. Predicted and experimental fracture toughness of single crystal tungsten for 5 strain rates. The experimentally measured transition temperatures [13] are marked with vertical dotted lines.

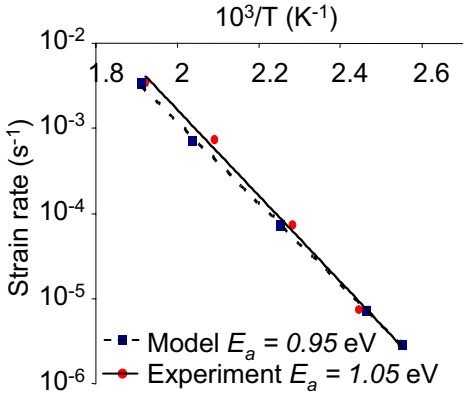

Figure 5. Arrhenius plot of experimental and predicted transition temperatures. The net activation energy resulting from the model is in excellent agreement with the experimental value.

the material does fracture as the dislocation shielding is reduced and the fracture condition (1) is met at $K_{tip} = K_{Ic}$. This value of v_0 $(5.8 \times 10^5 \mathrm{ms}^{-1})$ was then used to simulate fracture tests at higher strain rates.

Figure 4 shows the predicted and experimental fracture toughness K_{frac} as a function of temperature at five different strain rates, corresponding to values used in the experiments [13] (the strain rate quoted is that on the tensile surface). The model reproduces the variation of K_{frac} with increasing T, the rapid rise in K_{frac} close to the BDT and the increase in T_{BDT} resulting from increased strain rates (see Table 1).

Experiments show that an empirical relation is valid for the strain rate depen-

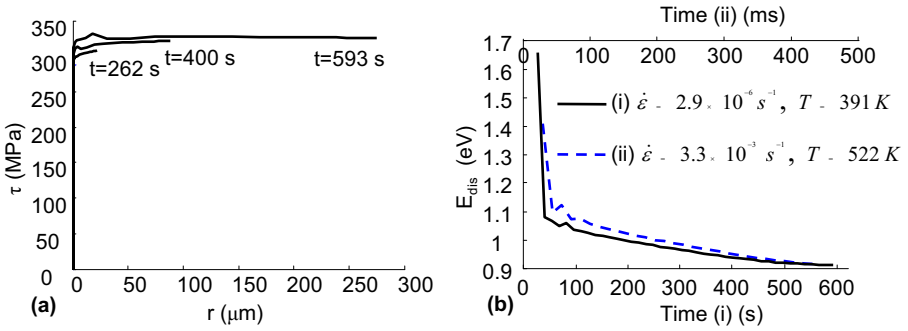

Figure 6. (a) Resolved shear stress felt by dislocations as a function of time and dislocation position, for $\dot{\varepsilon} = 2.9 \times 10^{-6} s^{-1}$, $T = 391$ K. (b) The activation energy of dislocations as a function of time at $\dot{\varepsilon} = 2.9 \times 10^{-6} s^{-1}$, $T = 391$ K and $\dot{\varepsilon} = 3.3 \times 10^{-3} s^{-1}$, $T = 522$ K.

dence of the BDT in a wide range of materials,

$$\dot{\varepsilon} = \varepsilon_0 \exp(-E_a / k_B T_{BDT}), \tag{9}$$

where T_{BDT} is the measured transition temperature at strain rate $\dot{\varepsilon}$ and ε_0 is a constant. Plotting $\ln \dot{\varepsilon}$ against $1/T_{BDT}$ produces a straight line with a gradient equal to the activation energy of the BDT. The predicted and experimental transition temperatures are plotted in Arrhenius form in figure 5. The data from the model lie on a straight line covering the whole range of $\dot{\varepsilon}$, yielding an activation energy of 0.95 eV. The activation energy is considerably lower than the kink-pair energy, Q (1.75 eV); but is consistent with that measured experimentally. The net activation energy for motion of the dislocations in the mobility law (5) is $E_{dis} = Q - \tau V_A$, with $Q = 1.75$ eV and $V_A = 20b^3$. The dislocations in the crack-tip arrays self-organise under the influence of the applied stress and their elastic interactions so that, at conditions close to the BDT, the net stresses on the dislocations are approximately constant with time and with dislocation position. This is because the dislocation velocity law depends strongly (exponentially) on the stress. This strong coupling between dislocation motion and stress causes a dislocation to quickly accelerate if it feels a force pushing it forward from the dislocation behind it and slow down again as it approaches the dislocation in front of it; this results in the dislocations forming a dynamic 'pile up' moving at constant speed. Figure 6 a) shows the resolved stress τ in the dislocation array, calculated using (4). The stress is very nearly constant in the array at all times and positions, and is 326 MPa at all the predicted transition temperatures. Figure 6(b) shows the resultant net activation energy, E_{dis}, for two strain rates. At fracture $E_{dis} = 1.75$ eV $- 0.85$ eV ≈ 0.95 eV. This is equal to E_a obtained from figure 5.

3. Summary

We have applied a simple discrete dislocation dynamics model to crack-tip plasticity in fracture tests and found that the dislocation shielding can delay and even prevent fracture. This occurs because the dislocation shielding rate continually increases whereas the applied loading rate is constant, causing the stress intensity at the crack tip to peak and then decrease with increasing time. If this maximum in crack tip stress intensity K_{tip} is below K_{Ic} fracture cannot occur; this happens at high simulated temperatures, with associated high dislocation velocities and nucleation rates. If the strain rate is increased the applied deformation rate, $\dot{K}_{app}$ increases; to prevent fracture $\dot{K}_{dis}$ needs to increase and so the temperature needs to increase.

The predicted form of the brittle-ductile transition and the increase in T_{BDT} with strain rate are in excellent agreement with experiments.

The model is 2D and consists of only two symmetrically placed slip planes in the presence of a straight sharp crack. However the model has also been examined with multiple slip planes parallel to those included here and the behaviour was not significantly different as the plastic flow was found to be concentrated on the slip planes intersecting the crack tip [20], furthermore EBSD images, see figure 2, indicate the majority of dislocation activity occurs on slip planes intersecting the crack-tip.

Crack-tip blunting due to dislocation emission is not included in this model. To do so would require the stress field around a blunted crack to be found in closed form; recent analytic work [21] may mean that this could be incorporated in the future. The blunting effect would be expected to scale with the number of dislocations emitted, the same scaling as that governing shielding. The inclusion of blunting effects would reduce the pre-factor B in (7) thereby reducing the dislocation shielding term, K_{dis}; the net effect would be that the same behaviour would be produced by the model but at a higher value of v_0.

The simulations use a velocity law based on kink-pair formation with an activation energy reduced by local shear stresses. The dislocations self-organise due to their mutual elastic interactions so that the shear stress in the dislocation array is effectively constant with time and position. This reduces the net activation energy for dislocation motion below that for kink pair nucleation. The activation energy, E_a, obtained from an Arrhenius plot of the predicted transition temperatures was found to be in very close agreement with the net activation energy for the dislocation motion, E_{dis}.

Where data are available, the activation energy for brittle-ductile transitions in various materials is identical with that for dislocation glide [22]. This suggests that the nucleation of dislocations at crack-tips is easy, and not the controlling factor in determining the BDT; it is the subsequent dislocation motion by glide away from the sources to 'make room' for more dislocations to be produced which dictates the fracture mode. This is consistent with the modelling results presented in this paper, and their good fit to experimental data.

Acknowledgements

We thank Dr J. Murphy for providing the image shown in figure 2. We also thank Dr. A. Giannattasio who provided the experimental fracture test data. We thank EPSRC for financial support under the research grant GR/M058811.

References

[1] F.C. Serbena and S.G. Roberts, *The brittle-ductile transition in germanium*, Acta. Metall. Mater. 42 (1994), pp. 2505–2510.
[2] P. Gumbsch, J. Riedle, A. Hartmaier, and H.F. Fischmeister, *Controlling factors for the brittle-to-ductile transition in tungsten single crystals*, Science 282 (1998), pp. 1293–1295.
[3] M. Brede and P. Haasen, *The brittle-to-ductile transition in doped silicon as a model substance*, Acta. Metall. 36 (1988), pp. 2003–2018.
[4] K.F. Ha, C. Yang, and J.S. Bao, *Effect of dislocation density on the ductile-brittle transition in bulk Fe - 3%Si single crystals*, Scripta. Metall. Mat. 30 (1994), pp. 1065–1070.
[5] S.G. Roberts, P.B. Hirsch, A.S. Booth, M. Ellis, and F.C. Serbena, *Dislocations, cracks and brittleness in single crystals*, Physica Scripta T49 (1993), pp. 420–426.
[6] B. Devincre, L.P. Kubin, C. Lemarchand, and R. Madec, *Mesoscopic simulations of plastic deformation*, Mat. Sci. Eng. A 309–310 (2001), pp. 211–219.
[7] V. Lakshmanan and J.C.M. Li, *Edge dislocations emitted along inclined planes from a mode I crack*, Mat. Sci. Eng. A 104 (1988), pp. 95–104.

[8] P.B. Hirsch, S.G. Roberts, and J. Samuels, *The brittle-ductile transition in Silicon - II. Interpretation*, Proc. R. Soc. Lond. A. 421 (1989), pp. 25–53.
[9] P.B. Hirsch, S.G. Roberts, and J.F. Nye, *Modelling crack tip plastic zones and the brittle-ductile transition*, Phil. Trans. Roy. Soc. 355 (1997), pp. 1991–2001.
[10] S.G. Roberts, *Modelling the brittle to ductile transition in single crystals*, in *Computer Simulation in Materials Science - nano/meso/macroscopic space and time scales*, H.O. Kirchener, L.P. Kubin and V. Pontikis, eds., NATO ASI series, series E, 308, Kluwer Academic Publishers, The Netherlands, 1996, pp. 409–434.
[11] ———, *Modelling Brittle-Ductile Transitions*, in *Multiscale Phenomena in Plasticity: from Experiments to Phenomenology, Modelling & Materials Engineering* J.L. et al. ed., Kluwer Academic Press, The Netherlands, 2000, pp. 349–364.
[12] M. Tanaka, E. Tarleton, and S.G. Roberts, *The brittle-ductile transition in single-crystal iron*, Acta Mater. 56 (2008), pp. 5123–5129.
[13] A. Giannattasio and S.G. Roberts, *Strain-rate dependence of the brittle-to-ductile transition temperature in tungsten*, Phil. Mag. 87 (2007), pp. 2589–2598.
[14] N. Urabe and J. Weertman, *Dislocation mobility in potassium and iron single crystals*, Mat. Sci. Eng. 18 (1975), pp. 41–49.
[15] J.P. Hirth and J. Lothe *Theory of dislocations*, Wiley-Interscience Publication, 1982.
[16] D. Brunner, *Comparison of flow-stress measurements on high-purity tungsten single crystals with the kink-pair theory*, Mater. Trans. JIM. 41 (2000), pp. 152–160.
[17] J.W. Christian and B.C. Masters, *Low-temperature deformation of body-centred cubic metals. I. yield and flow stress measurements*, Proc. R. Soc. Lond. Ser A 281 (1964), pp. 223–239.
[18] D. Brunner and V. Glebovsky, *Analysis of flow-stress measurements of high-purity tungsten single crystals*, Mat. Lett. 44 (2000), pp. 144–152.
[19] L. Vitos, A.V. Ruban, H. Skriver, and J. Kollar, *The surface energy of metals*, Surf. Sci. 411 (1998), pp. 186–202.
[20] I.M. Robertson, D.H. Lassila, B. Devincre and R. Philips (eds.), *MRS Proceedings*, Vol. 578, *A multi slip plane model for crack-tip plasticity*, Materials Research Society, Warrendale, PA, USA, 2000, pp. 309–314.
[21] T. Li and Z. Li, *The stress intensity factor of an edge dislocation near an elliptically blunted crack tip*, Int. J. Fract. 144 (2007), pp. 45–52.
[22] A. Giannattasio, M. Tanaka, T.D. Joseph, and S.G. Roberts, *An empirical correlation between temperature and activation energy for brittle-to-ductile transitions in single-phase materials*, Phys. Scr. T128 (2007), pp. 87–90.